Carotid Plaque 3D Compound Imaging and Echo-Morphology Analysis: a Bayesian Approach

J.C. Seabra (MSc), J.M. Sanches (PhD), L.M. Pedro (MD) and J.F. e Fernandes (MD)

***Abstract*—This paper describes a method for volume reconstruction of the carotid plaque and presents a novel local characterization of its echo-morphology. The data is composed by a series of nearly parallel ultrasound images (3D Compound Imaging) and the acquisition is performed using traditional non-invasive ultrasound equipment available in most medical facilities, without need of a spatial locator device. The reconstruction algorithm uses the observed pixels inside the plaque, which were obtained in a pre-segmentation stage performed under medical guidance [1].**

The paper proposes a Bayesian algorithm which estimates the underlying volume inside the plaque, by filtering and interpolating the data in order to remove speckle noise and fill non-observed regions, respectively. This volume is further used in plaque echo-morphology analysis.

The observation model is based on the Rayleigh distribution, commonly used to model speckle noise in ultrasound images. A prior model based on the edge preserving Total Variation Gibbs distribution is also used to fill the gaps on non-evenly spaced observations. An energy function is derived from these models and an iterative algorithm computes its minimizer.

The estimated function, defined in a given volume of interest, is used in global and local plaque characterization, namely to estimate its average levels of stenosis, echo-morphology and to identify vulnerable *foci* inside the plaque. The goal is to make atherosclerosis diagnosis more accurate and complete than using traditional 2D ultrasound analysis.

I. INTRODUCTION

Carotid atherosclerosis is one of the main causes of stroke which is the most common life-threatening neurological disease. Its most important feature is plaque formation due to accumulation of lipid, protein, and cholesterol esters [2]. These plaques cause a gradual thickening (stenosis) of the arterial lumen making the blood flow to the brain more difficult. The risk of stroke increases with the severity of carotid stenosis and decreases after endarterectomy, i.e. plaque removal. Up to now the degree of stenosis has been targeted as a strong predictor of stroke [3]. Indeed, it is the only criterion used to decide about a surgical intervention.

Because the decision for surgical intervention presents important clinical and financial consequences, a relevant effort is being done in the study of new diagnostic tools and indicators of plaque risk, namely, by using ultrasound (US) imaging. US is non-invasive, easily accessible, acquires in real time and is less expensive than other imaging modalities (MRA or CT). Studies using US encompass a broad range of techniques to measure stenosis severity or intima-media layer thickness and to characterize the plaque echogenicity and texture through parameters such as the gray scale median (GSM), variance or percentile of echolucent pixels (P40) [4].

However, the assessment of plaque risk through conventional two-dimensional (2D) techniques may not be very accurate because it is limited to a subjective selection of a particular US image which needs to be representative of the plaque structure. Moreover, since a single and precise cutting plane is difficult to reproduce, an accurate monitoring of disease progression is also arduous to perform.

By this, new methods based on 3D US have been proposed [5], where reconstructed volumes are used to better assess plaque vulnerability. 3D US uses a conventional transducer, manipulated mechanically or free-handed, to produce serial planar cross-sections at different spatial positions and orientations. Usually, in both cases, a spatial locator is attached to the probe to measure its location. However, these devices are expensive and not usually available.

Two approaches are usually considered to describe the carotid and plaque geometries in a certain region of interest (ROI): surface rendering and volume rendering.

In the first approach, realistic models of the carotid bifurcation are created and used to quantify the level of stenosis and plaque volume [6]. The second approach is used, for instance, to assess surface ulceration [7]. Plaque morphology, based on specific statistical parameters, is being used to characterize plaque echogenicity and texture. However, these global measures may not be sufficient and accurate in most cases. In [1] is described a computational tool for plaque analysis based either on surface and volume reconstruction. The estimated carotid wall and plaque geometries are obtained by extracting their contours from the US images using active contours, and the plaque characterization is done by making statistical analysis of the non equally spaced noisy observations obtained from its interior.

In this paper, non-evenly spaced noisy observations are used in a Bayesian framework to estimate the underlying continuous function which is thereafter used to compute statistical parameters that describe plaque echo-morphology. The continuous function is used to locally characterize the plaque as well as to compute relevant global parameters, such as the level of stenosis and the plaque volume.

The next section refers to the problem description. Section 3 describes the algorithm used for plaque reconstruction and characterization. Section 4 presents experimental results with medical validation and discussion, and section 5 concludes the paper.

This work was supported by Fundação para a Ciência e a Tecnologia (ISR/IST plurianual funding) through the POS Conhecimento Program which includes FEDER funds.

J. Seabra and J. Sanches are with Institute of Systems and Robotics, Technical University of Lisbon, Portugal jseabra@isr.ist.utl.pt

L.M. Pedro and J. Fernandes e Fernandes are with Cardiovascular Institute of Lisbon, Faculty of Medicine, Portugal

II. PROBLEM DESCRIPTION

The data used to reconstruct the middle region of the carotid artery, near the bifurcation where the plaque formation is more frequent, is composed of a set ($n = 60$) of nearly parallel cross-sections (fig. 1(a)). Since no spatial locators are being used, the acquisition protocol is a critical process to guarantee the quality of results. Here, it is used an acquisition protocol described in [1] where it is reported that reconstruction errors due to variations on probe velocity and orientation are not relevant. In this previous work, the authors proposed a semi-automatic segmentation algorithm to build realistic 3D meshes of the carotid and plaque. These meshes are obtained from the contours extracted from the US images by using active contours, under medical supervision. This contours are smoothed, linked and aligned and and thereafter used in mesh reconstruction process.

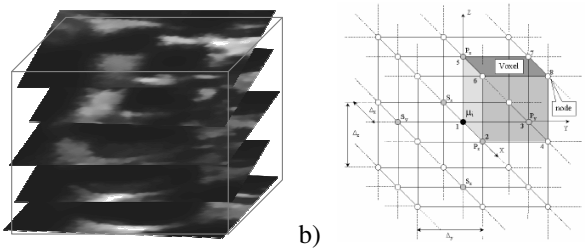

Fig. 1. 3D reconstruction scheme. a) 3D Compound Imaging. b) 3D regular grid used for volume reconstruction.

In the current work, the data to be processed is composed by the pixels inside the plaque obtained from the previous segmentation process. However, this data presents some undesirable features: 1) is noisy, being corrupted by a type of multiplicative noise called *speckle*; 2) is sparse, because there are few cross sections covering the plaque regions (only about 20) which may not observe all region of interest and 3) is not evenly spaced, because the alignment algorithm must compensate for the variations in the orientation and velocity of the US probe and for tissue movement and deformation during acquisition process.

The speckle noise is generated during the acquisition process and is caused by the interaction of acoustic waves with biological tissues and probe surface. The analysis of the physics associated with US propagation suggests that the received echo can be modeled by a Rayleigh distribution [8].

In this paper, a Bayesian approach with a *Maximum a Posteriori* (MAP) criterion is used to estimate a continuous function $f : \Omega \rightarrow R$, with $\Omega \in R^3$, describing the underlying volume inside the plaque, from a set of observations, $Y = \{y_i\}$ and corresponding positions $X = \{x_i\}$,

$$\hat{F} = \arg\max_F J(Y, X, F), \tag{1}$$

where $J(Y, X, F) = \log(p(Y|F, X)p(F))$ is an objective function, F is a vector column of coefficients defining $f(x)$, $p(Y|F, X)$ is the observation model and $p(F)$ is an edge preserving Gibbs prior distribution used to regularize the solution, by filling the gaps and remove the speckle noise. The function $f(x)$ to be estimated is defined as a linear combination of basis functions, $f(x) = F^T\Phi(x)$ where $\Phi(x) = [\phi_0(x), \phi_1(x), ..., \phi_{N-1}(x)]^T$ is a column vector of basis functions, $\phi_k(x)$, centered at the nodes of a 3D regular grid (see Fig.1(b))

It is assumed statistical independence of the observations, leading to the following likelihood function

$$p(Y|F, X) = \prod p(y_i|F, x_i), \tag{2}$$

where

$$p(y|F, x) = \frac{y}{f(x)} e^{-\frac{y^2}{2f(x)}} \tag{3}$$

is the Rayleigh distribution. The prior function is an edge preserving *total variation* (TV) based Gibbs distribution [9] needed to interpolate the data and fill the gaps without distorting the transitions,

$$p(F) = \frac{1}{Z} e^{-\alpha \sum g_k} \tag{4}$$

where g_k is the gradient magnitude of $f(x)$, $|\nabla f(x)|$, computed at kth node. This gradient magnitude can be approximated as follows

$$g_k = \sqrt{\sum_{j=1}^{6} (f_k - f_{k_j})^2} \tag{5}$$

where f_{k_j} are the six neighbors of f_k. The α parameter is used to control the strength of the connections among neighboring nodes and is manually tunned. High values of α lead to cleaner and smoothed solutions and smaller values of α lead to better preserved detail solutions but also noisier. The parameter α is also used here to implement a continuation method to improve the convergence properties of the algorithm. In this method the α parameter assumes large values in the first steps of the reconstruction process being gradually reduced along the iterations.

III. RECONSTRUCTION AND CHARACTERIZATION

The maximization of (1) is done by finding the stationary point of $J(Y, X, F)$, $U(Y, X, F) = \nabla_F J(Y, X, F) = 0$, with the Newton-Raphson method. In a element wise basis,

$$\frac{\partial}{\partial f_k} \log p(Y|F) + \frac{\partial}{\partial f_k} \log p(F) = 0, \tag{6}$$

Differentiating each term with respect to f_k yields to

$$\frac{\partial}{\partial f_k} \log p(Y|F) = \frac{1}{2} \sum \frac{2f(x_i) - y_i^2}{f^2(x_i)} \phi_k(x_i) \tag{7}$$

$$\frac{\partial}{\partial f_k} \log p(F) = \frac{6\alpha}{g_k} [f_k - \overline{f_k}] \tag{8}$$

where $\overline{f_k} = \frac{1}{N_V} \sum f_{k\tau}$. Replacing (7) and (8) in (6) and considering the approximation $f(x_i) \approx f_k$ leads to:

$$\frac{1}{f_k} \sum \phi_k x_i - \frac{1}{2f_k^2} \sum y_i^2 \phi_k(x_i) + \frac{6\alpha}{g_k} (f_k - \overline{f_k}) = 0 \tag{9}$$

The element wise Newton-Raphson method is formulated as follows

$$f_k^{t+1} = f_k - \frac{U(y_k, x_k, f_k)}{\partial U(y_k, x_k, f_k)/\partial f_k}, \tag{10}$$

where

$$U(y_k, x_k, f_k) = \frac{b_k}{f_k} - \frac{f_k^{ML}}{f_k^2} + \frac{6\alpha}{g_k}(f_k - \overline{f}_k) \quad (11)$$

where $b_k = \sum_{i \in V_k} \phi_k(x_i)$ and $f^{ML} = \frac{1}{2}\sum y_i^2 \phi_k(x_i)$ is the maximum likelihood (ML) estimate.

Equation (10) can be rewritten as follows

$$f_k^{t+1} = f_k \frac{\frac{6\alpha\overline{f}_k}{g_k} f_k^2 - 2 f_k b_k + 3 f_k^{ML}}{\frac{6\alpha\overline{f}_k}{g_k} f_k^3 - b_k f_k + 2 f_k^{ML}}. \quad (12)$$

The initialization is performed with $F^{ML} = \{f_k^{ML}\}$ and the stop criterion is the norm of the error, that is, $E = ||F^t - F^{t-1}||$. In non-observed regions, the 3D grid F^{ML} is filled with the Rayleigh mean value of whole plaque observations.

The statistics needed to characterize the echogenicity and texture are computed from the estimated $f(x)$ according to theoretical estimators derived from the Rayleigh distribution. For instance, estimators for the mean (μ), standard deviation (σ), median (υ) and percentile 40 (P40) for the Rayleigh distribution with parameter $f(x)$ are the following

$$\mu = \sqrt{\frac{\hat{f}(x)\pi}{2}} \quad (13)$$

$$\sigma(x) = \sqrt{\frac{4-\pi}{2}\hat{f}(x)} \quad (14)$$

$$\upsilon(x) = \sqrt{2\log(2)\hat{f}(x)} \quad (15)$$

$$P40(x) = 1 - e^{\frac{-40^2}{2\hat{f}(x)}}. \quad (16)$$

These estimators will be used to continuously ($x \in R^3$) characterize the plaque echo-morphology.

IV. Experimental Results and Discussion

In this section experiments using synthetic and real data will be displayed. Fig. 2 shows the results using synthetic data. This volume is composed by a white cylinder ($f(x) = 0.75$) inside an homogeneous region ($f(x) = 0.25$). A $96 \times 96 \times 96$ dimension 3D grid is used to represent $f(x)$ and the reconstruction algorithm associates each estimated coefficient f_k to a node of the grid.

The set of images ($n = 50$) extracted from the original and noiseless volume, are artificially corrupted by multiplicative noise with Rayleigh distribution. Fig. 2(a) shows a noiseless cross-section of the original object and the corresponding image corrupted by noise (Fig. 2(b)). Figs. 2(c)-(d) show the ML estimation, $f^{ML}(x)$, from which the MAP algorithm is initialized, and the MAP solution, $f^{MAP}(x)$. The corresponding surface profiles are displayed in Figs. 2(e)-(f). It is observed a regularization effect produced by the prior contribution. Figs. 2(g)-(h) illustrate the 3D reconstructions using a volume rendering visualization approach.

The second set of tests uses real data composed by $n = 60$ cross sections of a carotid artery of a patient with atherosclerosis. The results are depicted in fig. 3. Figs. 3(a)-(b) are cutting planes of the ML and the MAP estimates from the observed data. Figs. 3(c)-(d) show the respective surface profiles and

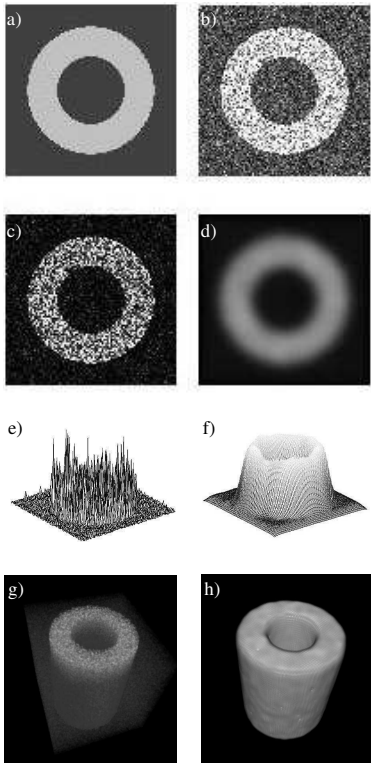

Fig. 2. Synthetic results. a-b) True and noisy cutting planes, c-d) ML and MAP estimates of f_k, e-f) Surface meshes of ML and MAP and g-h) 3D visualizations with volume rendering.

Figs. 3(e)-(f) present the volume reconstructions of both ML and MAP estimates. There is similarity between the two images and the observed data, except for some regularization and blurring effects, specially at the transitions.

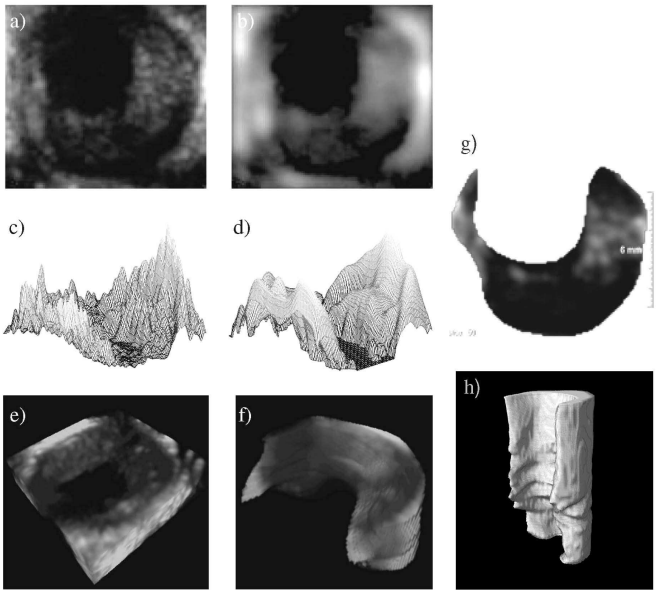

Fig. 3. Real results. a-b) ML estimate of the original (noisy) cutting plane and the corresponding MAP estimate of f_k, c-d) Surface profiles of ML and MAP, e-f) 3D visualizations with volume rendering. g) Virtual cross-section of the carotid plaque. h) Plaque surface, showing irregularities.

With this method is possible to extract virtual cross-sections (Fig. 3(g)) with arbitrary positions and orientations without need of the physical presence of the patient, allowing a more accurate and complete inspection of the carotid plaque. Using a region growing algorithm, plaque morphology in 3D is segmented (Fig. 3(h)). Other important feature consists in its continuous characterization by using statistical estimators given by (13)-(16). Table I shows a close similarity between the statistical parameters determined by the medical doctor and those obtained with the estimated function $\hat{f}_k$. With this functionality is possible to detect vulnerable plaque regions by using different statistical measures.

TABLE I
GLOBAL CHARACTERIZATION OF CAROTID PLAQUE ECHO-STRUCTURE

Parameters	2D medical	Parameters	3D estimated
μ_{y_o}	44.29	$\overline{\hat{f}}_{\mu}$	49.31
υ_{y_o}	40	$\overline{\hat{f}}_{\upsilon}$	46.33
σ_{y_o}	27.83	$\overline{\hat{f}}_{\sigma}$	25.78
$P40_{y_o}$	50.62	$\overline{\hat{f}}_{P40}$	56.76

The analysis of plaque echo-morphology, in particular the GSM (or median) and P40 (percentage of hypoechogenic voxels) determines whether (or not) the plaque is stable, considering the consensual thresholds given in the literature: $GSM < 32$ and $P40 > 43$ [4]. This binary classification is, however, very simple and incomplete as it can give rise to wrong diagnostic and clinical decisions, because it does not give any information about the extension of the unstable regions inside the plaque.

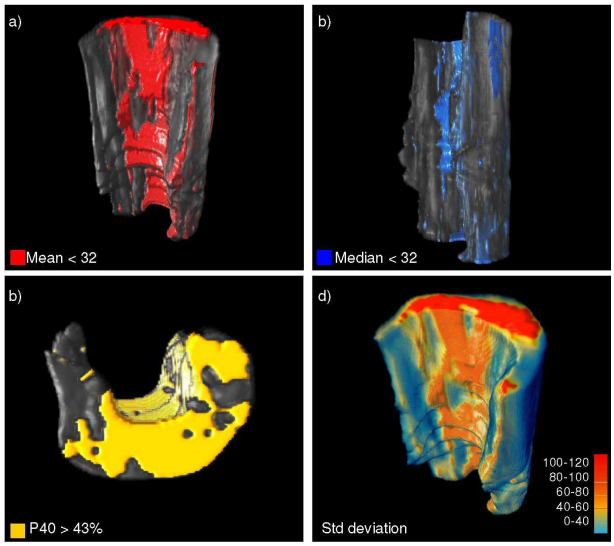

Fig. 4. Local assessment of plaque echo-morphology, in terms of: a-c) hypoechogenicity and d) heterogeneity.

A local characterization is clinically relevant to obtain information about plaque local echo-morphology which is not provided by global measurements. Fig.4 displays results of the local analysis using different statistical-based criteria. Figs.4(a)-(c) show the identification of regions of hypoechogenicity, with mean and median values below 32 and P40 above 43%. These are typically related to the presence of lipid, hemorrhage, inflammatory activity and thus instability. Moreover, Fig. 4(d) shows results of a measure of plaque texture, assessed with the standard deviation [10].

V. CONCLUSIONS

A 3D reconstruction algorithm was presented, based on a Bayesian approach, assuming a Rayleigh model describing the observation data and a TV prior. The use of the Rayleigh model is justified by the image formation process and the presence of speckle noise. The algorithm was tested using synthetic and real data. Good results were achieved in both cases, regarding noise reduction and data interpolation from non equally spaced observations.

3D compound imaging of the carotid plaque is addressed towards its morphological characterization in a local basis. This issue may have clinical relevance on the diagnosis and treatment of the disease, since traditional studies either performed in two dimensions or/and assessing plaque global echo-structure (global GSM and P40) show variability and are not sufficient. Analysis of plaque composition is performed by computing a set of statistical estimators, such as mean, median, P40 and standard deviation for each spatial position of the carotid plaque data. Plaque echogenicity is assessed by detecting the more hypoechogenic regions within the plaque, considering thresholds presented in the literature. Texture is assessed by defining a colorscale of heterogeneity. This study leads to significant improvements on the current state-of-the-art atherosclerosis diagnosis tools. It can provide a more complete characterization of the carotid plaque and tracking of disease progression or response to treatment.

REFERENCES

[1] J. Seabra, J. Sanches, L. Pedro, and J. F. e Fernandes, "Three-dimensional ultrasonic assessment of atherosclerotic plaques," in *Proceedings of the IbPRIA Conference*, 2007.
[2] C. Zarins, C. Xu, and S. Glagov, "Atherosclerotic enlargement of the human abdominal aorta," *Elsevier Sc. Ireland*, pp. 157–164, 2001.
[3] E. C. for the Asymptomatic Carotid Atherosclerosis Study (ECAC), "Endarterectomy for asymptomatic carotid stenosis," *J. Am. Med. Assoc.*, vol. 8, pp. 273–1421, 1995.
[4] L. Pedro *et al.*, "Computer-assisted carotid plaque analysis: characteristics of plaques associated with cerebrovascular symptoms and cerebral infarction," *Eur J Vasc Endov Surg*, vol. 19, 2000.
[5] A. Fenster, D. B. Downey, and H. N. Cardinal, "Three-dimensional ultrasound imaging," *Phys. Med. Biol.*, vol. 46, no. 1, pp. 67–99, 2001.
[6] D. Barratt *et al.*, "Reconstruction and quantification of the carotid artery bifurcation from 3-d ultrasound images," *IEEE Transactions on Medical Imaging*, vol. 23, no. 5, May 2004.
[7] U. Schminke, L. Motsch, L. Hilker, and C. Kessler, "Three-dimensional ultrasound observation of carotid artery plaque ulceration," *Stroke*, vol. 31, no. 7, pp. 1651–1655, 2000.
[8] P. Shankar, "Speckle reduction in ultrasound b-scans using weighted averaging in spatial compounding," *IEEE Transactions on Ultrasonics, Ferroelectrics and Freq Control*, vol. 33, no. 6, pp. 754–758, 1986.
[9] J. Sanches, J. B. Dias, and J. Marques, "Minimum total variation in 3d ultrasound reconstruction," in *IEEE International Conference on Image Processing*, Genova, September 2005.
[10] L. Baroncini *et al.*, "Ultrasonic tissue characterization of vulnerable carotid plaque: correlation between videodensitometric method and histological examination," *Cardiov Ultrasound*, vol. 4, no. 32, 2006.